Biosensors and Bioelectronics 100 (2018) 577–582

Contents lists available at ScienceDirect

Biosensors and Bioelectronics

journal homepage: www.elsevier.com/locate/bios

Peptide-based electrochemical biosensor for juvenile idiopathic arthritis detection

V.R. Rodovalho[a], G.R. Araujo[a], E.R. Vaz[a], C. Ueira-Vieira[a], L.R. Goulart[a], J.M. Madurro[b], A.G. Brito-Madurro[a,*]

[a] Institute of Genetics and Biochemistry, Federal University of Uberlândia, Uberlândia, Brazil
[b] Institute of Chemistry, Federal University of Uberlândia, Uberlândia, Brazil

ARTICLE INFO

Keywords:
Biosensor
Mimetic peptide
Diagnosis
Screen-printed electrode
Juvenile idiopathic arthritis

ABSTRACT

Juvenile idiopathic arthritis (JIA) is a wide group of diseases, characterized by synovial inflammation and joint tissue damage. Due to the delay in the implementation of biomarkers into clinical practice and the association with severe sequels, there is an imperative need for new JIA diagnosis strategies. Electrochemical biosensors based on screen-printed electrodes and peptides are promising alternatives for molecular diagnosis. In this work, a novel biosensor for detecting juvenile idiopathic arthritis (JIA) was developed based on the immobilization of the PRF + 1 mimetic peptide, as recognition biological element, on the surface of screen-printed carbon electrode. This biosensor was able to discriminate the JIA positive and negative serum samples from different individuals using differential pulse voltammetry, presenting limits of detection and quantification in diluted samples of 1:784 (v/v) and 1:235 (v/v), respectively. Evaluation by electrochemical impedance spectroscopy showed R_{CT} 3 times higher for JIA positive sample than for a pool of human serum samples from healthy individuals. Surface analysis of the biosensor by atomic force microscopy, after contact with JIA positive serum, presented great globular clusters irregularly distributed. The long-term stability of the biosensor was evaluated, remaining functional for over 40 days of storage (after storage at 8 °C). Therefore, a simple, miniaturized and selective biosensor was developed, being the first one based on mimetic peptide and screen-printed carbon electrode, aiming at the diagnosis of the juvenile idiopathic arthritis in real serum samples.

1. Introduction

Juvenile idiopathic arthritis (JIA) is a wide set of autoimmune and inflammatory diseases that affect children and adolescents under the age of sixteen, mainly characterized by synovial inflammation and joint tissue damage (Abramowicz et al., 2016; Barut et al., 2017; Giancane et al., 2017; Hersh and Prahalad, 2015). JIA comprises distinct subtypes, from which oligoarticular, polyarticular and systemic are the most common (Dimitriou et al., 2017; Giancane et al., 2016). Diagnosis is essentially by exclusion, based on medical history, physical examination, imaging and serological tests, but implementation of biomarkers into clinical practice is often delayed (Consolaro et al., 2015; Dimitriou et al., 2017; Giancane, 2016).

The absence of a proper diagnosis and treatment for JIA may result in significant impacts on quality of life, including irreversible damage in the joint tissues, physical limitations, disfigurement and multiple sequels (Abramowicz et al., 2016; Consolaro et al., 2015; Giancane et al., 2016; Wipff et al., 2016). Hence, the development of new tools with potential to aid JIA diagnosis is of a high relevance to improve early detection and treatment.

Electrochemical biosensors emerge in the clinical scenario as promising analytical platforms. They are designed in diverse configurations, including conventional (Li et al., 2013; Liu et al., 2016), nanostructured (Pan et al., 2017; Pandey et al., 2017; Silva et al., 2013), polymer-modified (Castro et al., 2014; Dervisevic et al., 2017; Rodrigues et al., 2014) and screen-printed (Abbaspour and Noori, 2012; Chan et al., 2016) electrodes. In addition, the biomolecules most often employed as recognition elements are nucleic acids (Castro et al., 2014; Souza e Silva et al., 2016), enzymes (Pakapongpan and Poo-Arporn, 2017; Paraíso et al., 2014; Silva et al., 2013), antibodies (Pandey et al., 2017; Rodrigues et al., 2014) and peptides (Hwang et al., 2017; Li et al., 2013; Liu et al., 2016). Peptides have been increasingly employed as recognition elements in biosensors due to their relative stability against denaturation, chemical versatility, specificity and simple acquisition by natural sources, selection in random libraries and chemical synthesis (Liu et al., 2015; Pavan and Berti, 2012).

* Corresponding author.
E-mail address: agbrito@ufu.br (A.G. Brito-Madurro).

http://dx.doi.org/10.1016/j.bios.2017.10.012
Received 17 July 2017; Received in revised form 22 September 2017; Accepted 4 October 2017
Available online 05 October 2017

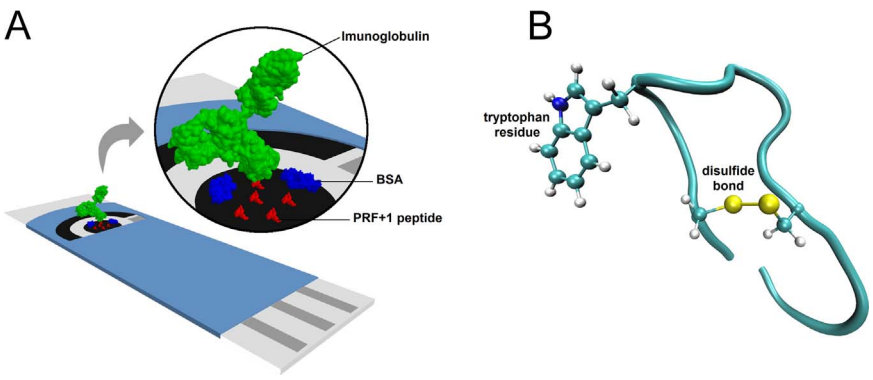

Fig. 1. Three-dimensional representations of the biosensor and its components. A) Biosensor (SPCE/PRF + 1/BSA) after application of positive serum sample, interacting with specific immunoglobulin related to JIA. B) Predicted structure of PRF + 1 peptide (ACSSWLPRGCGGGS), highlighting in balls-and-sticks the sidechains from amino acids reported to oxidize on carbon electrodes.

Screen-printed electrodes are produced by the deposition of a conductive film over an inert substrate and they present advantages such as serial production, low cost, rapid response, potential for automation and portability (Couto et al., 2016; Karunakaran et al., 2015). Their clinical use is increasing, with applications such as cancer diagnosis (Chan et al., 2016; Han et al., 2017) and pathogen detection (Abbaspour et al., 2015; Patris et al., 2016).

In a previous work, Araujo et al. (2016) selected peptides against antibodies purified from serum of JIA patients and assessed their performances for potential application in diagnosis. After validation, the synthetic PRF + 1 peptide was able to discriminate JIA patients from healthy individuals and patients with other immune-mediated rheumatic diseases with high accuracy. In the present work, we aimed to employ PRF + 1 peptide as a recognition biological element in the development of a simple, selective and sensitive platform for JIA detection. Therefore, screen-printed carbon electrodes (SPCEs) were modified with PRF + 1 peptide and tested for the differential recognition of JIA and healthy control serum samples from different individuals, followed by performance evaluation.

Biosensors applied to rheumatoid arthritis diagnosis have been described in the literature (Ahn et al., 2011; Bertok et al., 2015; Drouvalakis et al., 2008; Pang et al., 2015; Villa et al., 2011). However, they do not refer to JIA specifically or use mimetic peptide as probe immobilized onto SPCE.

To the best of our knowledge, this is the first biosensor based on peptide and screen-printed carbon electrode specifically designed to detect JIA in human serum samples.

2. Material and methods

2.1. Reagents and instrumentation

Reagents Na_2HPO_4, NaH_2PO_4 and NaCl (Neon); $K_4Fe(CN)_6.3H2O$ (Fluka), $K_3Fe(CN)_6$ (Acros Organics), KH_2PO_4 (Vetec), KCl (J.T. Baker) and $HClO_4$ (Reagen) were used as purchased. Solutions were prepared with deionized water (Gehaka, 18 MΩ cm) and bubbled with ultrapure N_2 prior to electrochemical measurements. Percloric acid solution was prepared at 0.5 mol L^{-1}. Buffer solutions were saline phosphate buffer (PBS, 0.01 mol L^{-1}, pH 7.4, containing 10 mmol L^{-1} NaCl) and phosphate buffer (PB, 0.1 mol L^{-1}, pH 7.4) with or without the addition of 10 mmol L^{-1} NaCl. Potassium ferrocyanide/ferricyanide solutions were prepared at 5 mmol L^{-1} or 0.1 mmol L^{-1} containing 0.1 mol L^{-1} KCl.

Previously selected PRF + 1 peptide (ACSSWLPRGCGGGS) (Araujo et al., 2016) was chemically synthetized (GenScript) and diluted in deionized water (1 μg mL^{-1}). Blocking solution was prepared with bovine serum albumin (BSA, Sigma-Aldrich, 96%) at 3% (m v^{-1}) in PBS. A pool of human serum samples from healthy individuals and patients who met the criteria for JIA subtypes (persistent oligoarticular; extended oligoarticular; rheumatoid factor-positive polyarticular; rheumatoid factor-negative polyarticular; and systemic) was obtained with the approval of Research Ethics Committee from the Federal University of Uberlândia, Minas Gerais, Brazil (number 685/09). Serum samples were used without dilution or diluted in phosphate buffer.

All electrochemical measurements were performed with a CHI 760C potentiostat (CH Instruments, USA) and DS110 screen-printed carbon electrodes (Dropsens, Spain). Electrochemical impedance spectroscopy experiments were performed with PGSTAT302N (Metrohm Autolab, The Netherlands) and ItalSens IS-C screen-printed carbon electrodes (Palmsens, The Netherlands). The SPCEs consisted of a carbon counter electrode, a carbon working electrode and a silver pseudo-reference electrode.

2.2. Biosensor preparation

Prior to use, screen-printed carbon electrodes (SPCEs) were electrochemically cleaned by cyclic voltammetry (from 0 to +0.8 V, 50 mV s^{-1}) in percloric acid solution (0.5 mol L^{-1}). Then, their surface was activated through chronoamperometry (−1.4 V, 300 s) in phosphate buffer (0.1 mol L^{-1}, pH 7.4), (adapted from Sahin and Ayranci, 2015). Immediately after activation, 2 μL of PRF + 1 solution (1 μg mL^{-1}) was applied onto the SPCE surface and the system was maintained at room temperature for 30 min. Next, 2 μL of blocking solution (BSA, 3%) was applied onto the SPCE/PRF + 1 surface and maintained at room temperature for 30 min. Finally, 2 μL of healthy control (HC) or juvenile idiopathic arthritis (JIA) serum sample was applied onto the biosensor surface (SPCE/PRF + 1/BSA) and maintained at room temperature for 30 min, in order to test its differential recognition (Fig. 1A). Between each step of preparation, the electrodes were rinsed with phosphate buffer. The specificity of the PRF + 1 probe was confirmed by voltammetry analysis, EIS measurements and AFM images.

2.3. Electrochemical measurements

Electrochemical measurements were performed after each step through differential pulse voltammetry in phosphate buffer solution (0.1 mol L^{-1}, pH 7.4), with potential ranging from +0.2 to +1.0 V, scan rate 40 mV s^{-1}, modulation amplitude 0.05 V, step potential 0.008 V, modulation time 0.06 s and interval time 0.2 s, using diluted sera (1:100, v/v). The same technique was applied using potassium ferrocyanide/ferricyanide solution (0.1 mmol L^{-1}) with 0.1 mol L^{-1} KCl, potential range from −0.2 to +0.5 V, scan rate of 40 mV s^{-1}, modulation amplitude 0.05 V, step potential 0.008 V, modulation time 0.06 s and interval time 0.2 s, using undiluted serum. Electrochemical impedance spectroscopy was conducted using potassium ferrocyanide/ferricyanide solution (5 mmol L^{-1}) with 0.1 mol L^{-1} KCl, open circuit potential, frequencies ranging from 100 kHz to 10 mHz, amplitude 10 mV and serum dilution 1:100.

2.4. Figures of merit of the biosensor

The biosensor performance was evaluated with varying dilutions of

JIA serum sample, in order to determine the sensitivity, limits of detection and quantification. A pool of positive serum samples was used without dilution or diluted 1:300, 1:100, 1:50, 1:35, 1:25, 1:10 in phosphate buffer (0.1 mol L^{-1}, pH 7.4). Undiluted serum samples from different individuals were also tested, including 2 healthy controls (HC1, HC2) and 5 JIA patients (JIA1, JIA2, JIA3, JIA4, JIA5). Finally, the biosensor performance was also evaluated after storage at 8 °C for 0, 5, 10, 20, 30 or 40 days. Electrochemical measurements were conducted through differential pulse voltammetry in potassium ferrocyanide/ferricyanide solution (0.1 mmol L^{-1}) with 0.1 mol L^{-1} KCl.

2.5. Atomic force microscopy

Surface analysis of the biosensor was acquired with a Shimadzu SPM-9600 atomic force microscope, using silicon cantilevers with constant force 10–130 N m^{-1} and resonant frequency of 204–497 kHz. Measurements were performed in non-contact mode, using undiluted sera.

2.6. Bioinformatics analysis

PRF + 1 isoelectric point (pI) was predicted by PepCalc.com tool (Lear and Cobb, 2016), its three-dimensional structure was predicted by I-Tasser suite (Yang et al., 2015) and refined by minimization, equilibration and production in 298.15 K with NAMD (Phillips et al., 2005) and VMD (Humphrey et al., 1996).

2.7. Statistics and data presentation

All experiments were performed in triplicate and numeric results are presented as arithmetic means ± standard deviation. For each measurement, a new SPCE was used. When applicable, voltammograms were subtracted from their base line (measured on support electrolyte only) and plotted with Origin 8. Peaks were corrected and analyzed with Peak Analyzer tool in Origin 8. The value of peak current variation (Δi_p) was measured as the peak height, whereas charge (Q) was measured as the area under the peak. Impedance spectra and equivalent circuits were analyzed with software Nova 1.10, atomic force microscopy final images were obtained with Gwyddion 2.45, bar charts and other graphs were constructed with GraphPad Prism 6.

3. Results and discussion

3.1. PRF + 1 probe immobilization

SPCE sensitized with PFR + 1 peptide was evaluated through atomic force microscopy (AFM) and differential pulse voltammetry (DPV), Fig. 2.

AFM images for the bare SPCE (Fig. 2A) and modified with PRF + 1 (Fig. 2B) indicate that the surface was modified with the probe peptide. Bare SPCE surface showed a rough aspect with root mean square roughness (R_q) of 30.16 ± 1.45 nm and SPCE/PRF + 1 image showed globular clusters homogeneously distributed and R_q = 25.18 ± 0.69 nm. The decrease in R_q values after PRF + 1 immobilization indicates an homogeneous surface coverage by the peptide, which levels the surface valleys and peaks (Arya et al., 2014; Enache et al., 2016; Ferreira et al., 2006).

DPV analysis shows the presence of well-defined oxidation peak at E_p = + 0.49 V, with Δi_p = 23.55 ± 1.55 μA for SPCE/PRF + 1 (Fig. 2C) using phosphate buffer as electrolyte. According to the literature (Enache and Oliveira-Brett, 2013), tryptophan and cysteine residues, present in the PRF + 1 sequence (A**C**SS**W**LPRG**C**GGGS), can be oxidized onto carbon electrodes

However, PRF + 1 structure prediction showed the proximity of the cysteine residues and indicated the presence of disulfide bond (Fig. 1B), which is an oxidized form of these residues (Enache and Oliveira-Brett, 2011a). Therefore, the oxidation peak in + 0.49 V is attributed to tryptophan residue oxidation (Enache and Oliveira-Brett, 2011b, 2013).

The peptide immobilization was also investigated through DPV in KCl solution (0.1 mol L^{-1}) containing potassium ferrocyanide/ferricyanide redox pair (0.1 mmol L^{-1}). We observed oxidation peaks at E_p = + 0.19 V, with Δi_p = 1.41 ± 0.13 μA for SPCE and E_p = + 0.01 V, with Δi_p = 21.59 ± 0.43 μA for SPCE/PRF + 1 (Fig. 2D) using ferrocyanide/ferricyanide redox pair. For SPCE, the oxidation peak was detected in the same potential as reported elsewhere for carbon electrodes (Ferreira et al., 2011). However, for SPCE/PRF + 1, there was a 15-fold increase in current intensity and a shift to more negative potentials, which are related to $Fe(CN)_6^{4-}$ anionic nature and positive charges in PRF + 1 (predicted isoelectric point of 8.49). Therefore, attractive interactions are established between the immobilized positively-charged peptide and the anionic redox molecule in solution, enabling the redox molecule to approach the electrode surface and facilitating the electron transfer. Analysis in phosphate buffer corroborates with these results, revealing an increase in the current signal for SPCE/PRF + 1 in comparison to bare SPCE.

3.2. Detection of specific-IgG in serum samples from JIA patients

Serum samples of patients with juvenile idiopathic arthritis (JIA) and healthy control (HC) were applied to the biosensor (SPCE/PRF + 1/BSA) to evaluate its selectivity (Fig. 3).

DPV conducted in phosphate buffer, pH 7.4, showed oxidation peaks with Δi_p = 6.47 ± 0.21 μA and Q = 27.48 ± 1.07 μC for SPCE/PRF + 1/BSA; Δi_p = 7.31 ± 0.37 μA and Q = 31.78 ± 1.42 μC for SPCE/PRF + 1/BSA/HC; Δi_p = 8.03 ± 0.18 μA and Q = 35.30 ± 0.38 μC for SPCE/PRF + 1/BSA/JIA (Fig. 3A).

An increase in current intensity for JIA serum samples was observed when compared to HC. That increase suggests an interaction between PRF + 1 (probe) and specific IgG (target) caused by accumulation of oxidizable amino acid residues onto the biosensor surface.

DPV recorded in potassium ferrocyanide/ferricyanide pair redox showed different profiles for the previous three groups: Δi_p = 5.82 ± 0.20 μA and Q = 16.85 ± 0.07 μC for SPCE/PRF + 1/BSA; Δi_p = 2.91 ± 0.03 μA and Q = 9.47 ± 0.50 μC for SPCE/PRF + 1/BSA/HC; Δi_p = 0.92 ± 0.05 μA and Q = 2.57 ± 0.02 μC for SPCE/PRF + 1/BSA/JIA (Fig. 3B). The application of HC and JIA serum samples resulted in a decrease in current response of about 50% and 84%, respectively. In addition, JIA serum sample causes shift to a more positive potential, consistent with the formation of new layers, blocking physically the electrode surface, limiting $Fe(CN)_6^{4-}$ diffusion and decreasing current response (Hennessey et al., 2009).

Electrochemical impedance spectra (EIS) recorded in potassium ferrocyanide/ferricyanide confirmed the previous results. The charge transfer resistance values obtained were 1.64 ± 0.06 kΩ for SPCE, 2.33 ± 0.23 kΩ for SPCE/PRF + 1/BSA, 2.76 ± 0.22 kΩ for SPCE/PRF + 1/BSA/HC and 6.75 ± 0.33 kΩ for SPCE/PRF + 1/BSA/JIA, being $\chi^2 = 10^{-3}$. The increase in the R_{CT} observed for the biosensor using positive sample was 3-fold higher in relation to the biosensor without the target, indicating an obstruction in $Fe(CN)_6^{4-}$ charge transfer reaction due to the peptide-antibody interaction (Fig. 3C).

Surface analysis using AFM in absence or presence of positive and negative target is indicated in Fig. 3(D-F). SPCE/PRF + 1/BSA/JIA presented great globular clusters irregularly distributed (Fig. 3F). These results are coherent, since HC serum samples are expected not to contain molecules capable of triggering great morphological alterations in the biosensor surface. On the other hand, JIA serum samples contain antibodies that could interact with the immobilized peptide, forming immunocomplexes clusters (Ferreira et al., 2006). The roughness values to SPCE/PRF + 1/BSA/JIA, SPCE/PRF + 1/BSA and SPCE/PRF + 1/BSA/HC were 83.42 ± 5.93 nm, 27.82 ± 1.67 nm and 28.58 = ± 0.76 nm, respectively.

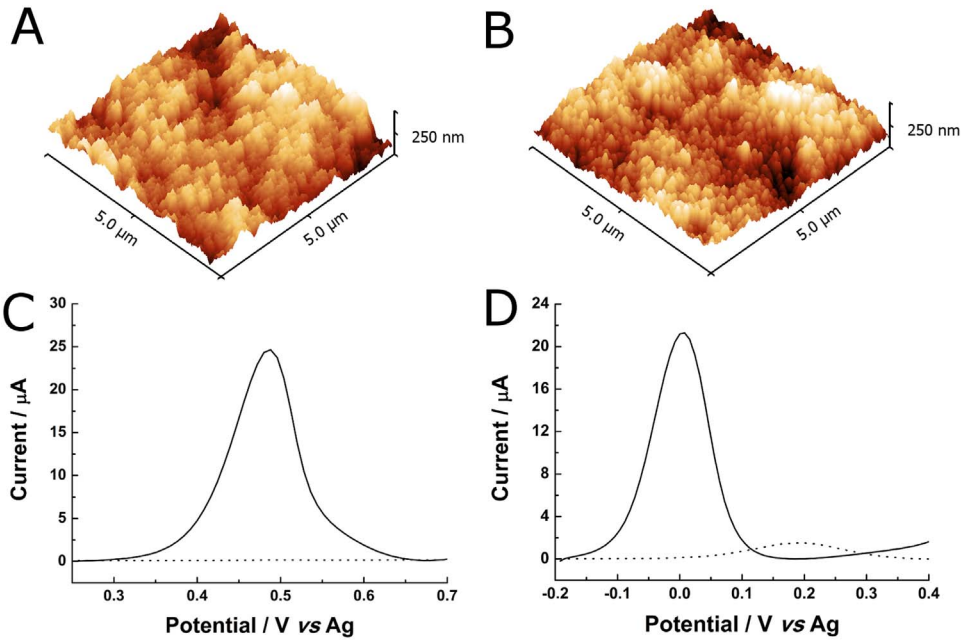

Fig. 2. AFM images for bare SPCE (A) and SPCE/PRF + 1 (B). Differential pulse voltammograms of bare SPCE (–) and SPCE/PRF + 1 (–) in 0.1 mol L^{-1} phosphate buffer (pH 7.4) (C) and 0.1 mmol L^{-1} potassium ferrocyanide/ferricyanide in 0.1 mol L^{-1} KCl (D).

3.3. Calibration curve

The biosensor response towards different dilutions of JIA serum sample was evaluated by differential pulse voltammetry in potassium ferrocyanide/ferricyanide redox pair (0.1 mmol L^{-1}) with 0.1 mol L^{-1} KCl (Fig. 4A).

The voltammograms show that the peak current intensity and dilution factor are directly proportional, since the peak current is higher for greater dilution factors (i.e., lower concentrations of JIA serum sample). As showed in Fig. 4B, the decrease in current intensity is justified by $Fe(CN)_6^{4-}$ diffusional barrier due to the interaction between PRF + 1 and IgG target. We observed a hyperbolic relationship with $r^2 = 0.9615$ From these data a linear relation of the charge values in function of the inverse of the dilution factor (1/DF) given by $Q = (-172.7 / FD) + 16.62$, $r^2 = 0.9989$ was found. The mean standard deviation of the data obtained was 2.6%. The sensitivity, limits of detection and quantification in diluted serum samples were 172.7 µC/µL, 1:784 and 1:235 respectively. Other studies detected specific targets in serum samples with higher dilution factors (Ding et al., 2005; Luna et al., 2014; Sharma et al., 2010; Souto et al., 2013; Wang et al., 2004). However, the dilution range presented here is enough for JIA diagnosis and supported by ELISA test (Araujo et al., 2016).

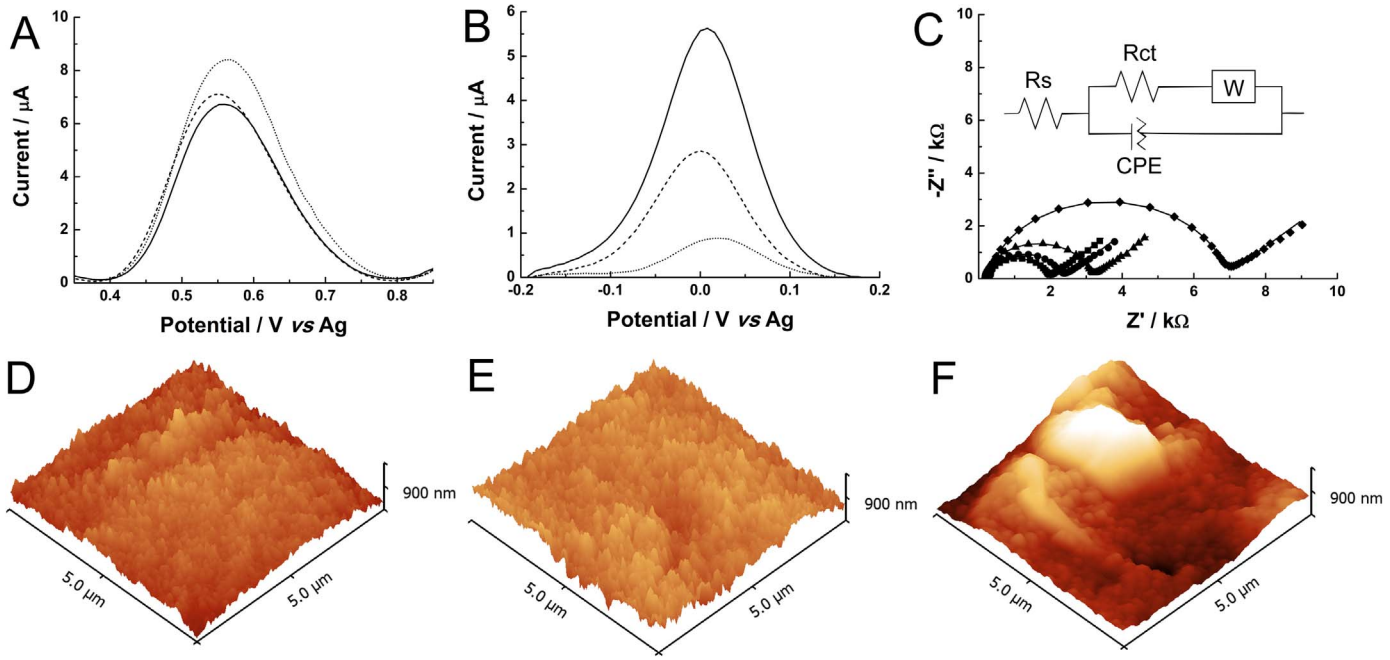

Fig. 3. Differential pulse voltammograms of SPCE/PRF + 1/BSA (---), SPCE/PRF + 1/BSA/HC (—) and SPCE/PRF + 1/BSA/JIA (···) in 0.1 mol L^{-1} phosphate buffer, pH 7.4 (A) and 0.1 mmol L^{-1} potassium ferrocyanide/ferricyanide in 0.1 mol L^{-1} KCl (B). Nyquist plots from electrochemical impedance spectroscopy in potassium ferrocyanide/ferricyanide (5 mmol L^{-1}) with 0.1 mol L^{-1} KCl (C) for: SPCE (■), SPCE/PRF + 1/BSA (•), SPCE/PRF + 1/BSA/HC (▲) and SPCE/PRF + 1/BSA/JIA (♦). Full lines represent fitting from equivalent circuit simulation. AFM images of SPCE/PRF + 1/BSA (D), SPCE/PRF + 1/BSA/HC (E) and SPCE/PRF + 1/BSA/JIA (F).

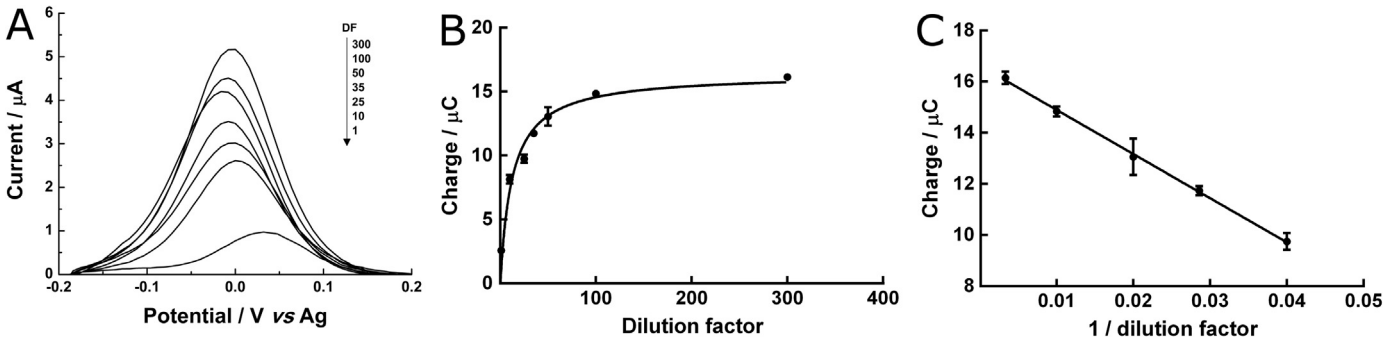

Fig. 4. Response of the biosensor in function of different dilutions of JIA serum sample. Differential pulse voltammograms recorded using the ferrocyanide/ferricyanide redox pair for different JIA serum sample dilution factors (1:300, 1:100, 1:50, 1:35, 1:25, 1:10) (A); Relation between charge and dilution factor (B) or the inverse of dilution factor (C).

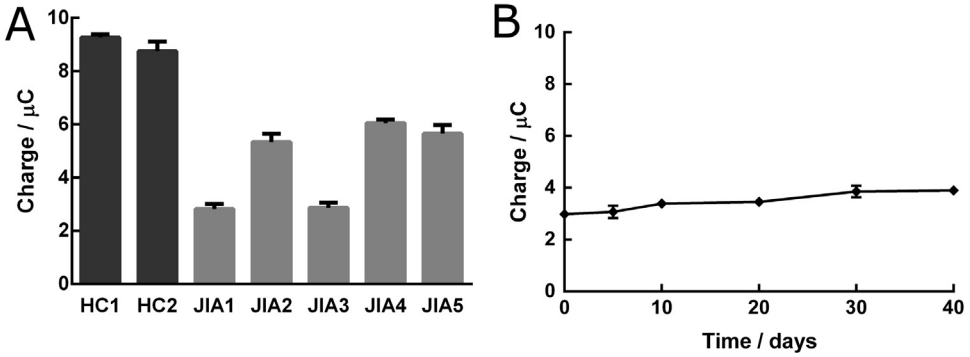

Fig. 5. Charge of the produced biosensor using samples from different patients with JIA (1–5) and healthy controls (HC1–HC2) (A). Stability of the biosensor after 0, 5, 10, 20, 30 and 40 days (B).

3.4. Patients variability test and stability of the biosensor

The biosensor capability of discriminating positive (JIA) and negative (HC) serum samples from different individuals was also studied, employing differential pulse voltammetry in potassium ferrocyanide/ferricyanide redox pair (Fig. 5A). The stability was monitored using DPV in potassium ferrocyanide/ferricyanide redox pair (Fig. 5B).

The results obtained using samples from different patients with JIA are in accordance with current response in Fig. 4B. There is greater variability among JIA patients, which is expected, due to diverse physiological, genetic, biochemical and psychological conditions. HC and JIA groups are efficiently discriminated by the produced biosensor and PRF + 1 was already shown to be efficient in JIA diagnosis by ELISA method (Araujo et al., 2016).

The charge response after 40 days of storage indicates that the biosensor maintained about 70% of its stability (Fig. 5B). Therefore, considering this result and storage conditions (dry, at 8 °C), the biosensor produced presents the desirable potential of long shelf-life. This stability is mainly due to the use of a peptide as recognition probe, since its tertiary structure is less complex than enzymes, antibodies and other proteins, being less susceptible to temperature, pH and ionic force fluctuations (Dover et al., 2009; Liu et al., 2015).

4. Conclusions

The PRF + 1 mimetic peptide used as recognition biological element for serum samples from positive patients for juvenile idiopathic arthritis was successfully immobilized onto screen-printed carbon electrode surface, and a 15-fold increase was observed in the current intensity when compared to bare electrode.

The biosensor developed enabled the discrimination of JIA and healthy controls, employing differential pulse voltammetry. The biosensor for juvenile idiopathic arthritis was reproducible, specific and detected until the dilution factor 1:784 (v/v) using real serum samples. In agreement with the analysis by VPD, electrochemical impedance spectroscopy showed R_{CT} 3 times higher for JIA positive sample than for the pool of human serum samples from healthy individuals. Surface analysis using AFM in the presence of JIA-positive target presented an increase in roughness values and great globular clusters irregularly distributed on the surface.

Therefore, a simple, miniaturized, functional, stable, selective and sensitive platform was developed and successfully applied to the detection of JIA in serum samples. This platform establishes itself as a promising analytical tool and joins the efforts to fill up the gap in JIA diagnosis. Future works should employ a higher number of patients, including samples from other inflammatory diseases, in order to validate the proposed platform for JIA diagnosis. Also, the regeneration of this platform can be tested as a way to reduce the cost to application in point of care.

Acknowledgements

The authors are grateful for the financial support from Conselho Nacional de Desenvolvimento Científico e Tecnológico (CNPq-306309/2015-7), Fundação de Amparo à Pesquisa do Estado de Minas Gerais (FAPEMIG/TEC - PPM-00378-12) and Coordenação de Aperfeiçoamento de Pessoal de Nível Superior (CAPES; master's *scholarship* for V. R. Rodovalho). Also, we would like to thank teacher *Abílio Borghi* for the review of the English manuscript.

References

Abbaspour, A., Noori, A., 2012. Electrochemical detection of individual single nucleotide polymorphisms using monobase-modified apoferritin-encapsulated nanoparticles. Biosens. Bioelectron. 37 (1), 11–18.

Abbaspour, A., Norouz-Sarvestani, F., Noori, A., Soltani, N., 2015. Aptamer-conjugated silver nanoparticles for electrochemical dual-aptamer-based sandwich detection of Staphylococcus aureus. Biosens. Bioelectron. 68, 149–155.

Abramowicz, S., Kim, S., Prahalad, S., Chouinard, A.F., Kaban, L.B., 2016. Juvenile arthritis: current concepts in terminology, etiopathogenesis, diagnosis, and management. Int. J. Oral Maxillofac. Surg. 45 (7), 801–812.

Ahn, K.Y., Kwon, K., Huh, J., Kim, G.T., Lee, E.B., Park, D., Lee, J., 2011. A sensitive diagnostic assay of rheumatoid arthritis using three-dimensional ZnO nanorod structure. Biosens. Bioelectron. 28 (1), 378–385.

Araujo, G.R., Fujimura, P.T., Vaz, E.R., Silva, T.A., Rodovalho, V.R., Britto-Madurro, A.G., Madurro, J.M., Fonseca, J.E., Silva, C.H., Santos, P.S., Mourao, A.F., Canhao, H., Goulart, L.R., Goncalves, J., Ueira-Vieira, C., 2016. A novel reactive epitope-based antigen targeted by serum autoantibodies in oligoarticular and polyarticular juvenile idiopathic arthritis and development of an electrochemical biosensor. Immunobiology 221 (5), 634–640.

Arya, S.K., Kongsuphol, P., Wong, C.C., Polla, L.J., Park, M.K., 2014. Label free biosensor for sensitive human influenza virus hemagglutinin specific antibody detection using coiled-coil peptide modified microelectrode array based platform. Sens. Actuators B: Chem. 194, 127–133.

Barut, K., Adrovic, A., Sahin, S., Kasapcopur, O., 2017. Juvenile idiopathic arthritis. Balk. Med. J. 34 (2), 90–101.

Bertok, T., Sediva, A., Filip, J., Ilcikova, M., Kasak, P., Velic, D., Jane, E., Mravcova, M., Rovensky, J., Kunzo, P., Lobotka, P., Smatko, V., Vikartovska, A., Tkac, J., 2015. Carboxybetaine modified interface for electrochemical glycoprofiling of antibodies isolated from human serum. Langmuir 31 (25), 7148–7157.

Castro, A.C.H., França, E.G., de Paula, L.F., Soares, M.M.C.N., Goulart, L.R., Madurro, J.M., Brito-Madurro, A.G., 2014. Preparation of genosensor for detection of specific DNA sequence of the hepatitis B virus. Appl. Surf. Sci. 314, 273–279.

Chan, K.F., Lim, H.N., Shams, N., Jayabal, S., Pandikumar, A., Huang, N.M., 2016. Fabrication of graphene/gold-modified screen-printed electrode for detection of carcinoembryonic antigen. Mater. Sci. Eng. C Mater. Biol. Appl. 58, 666–674.

Consolaro, A., Varnier, G.C., Martini, A., Ravelli, A., 2015. Advances in biomarkers for paediatric rheumatic diseases. Nat. Rev. Rheumatol. 11 (5), 265–275.

Couto, R.A., Lima, J.L., Quinaz, M.B., 2016. Recent developments, characteristics and potential applications of screen-printed electrodes in pharmaceutical and biological analysis. Talanta 146, 801–814.

Dervisevic, M., Dervisevic, E., Senel, M., Cevik, E., Yildiz, H.B., Camurlu, P., 2017. Construction of ferrocene modified conducting polymer based amperometric urea biosensor. Enzym. Microb. Technol. 102, 53–59.

Dimitriou, C., Boitsios, G., Badot, V., Lê, P.Q., Goffin, L., Simoni, P., 2017. Imaging of juvenile idiopathic arthritis. Radiol. Clin. North Am. 55 (5), 1071–1083.

Ding, Y., Wang, H., Shen, G., Yu, R., 2005. Enzyme-catalyzed amplified immunoassay for the detection of Toxoplasma gondii-specific IgG using Faradaic impedance spectroscopy, CV and QCM. Anal. Bioanal. Chem. 382 (7), 1491–1499.

Dover, J.E., Hwang, G.M., Mullen, E.H., Prorok, B.C., Suh, S.J., 2009. Recent advances in peptide probe-based biosensors for detection of infectious agents. J. Microbiol. Methods 78 (1), 10–19.

Drouvalakis, K.A., Bangsaruntip, S., Hueber, W., Kozar, L.G., Utz, P.J., Dai, H., 2008. Peptide-coated nanotube-based biosensor for the detection of disease-specific autoantibodies in human serum. Biosens. Bioelectron. 23 (10), 1413–1421.

Enache, T.A., Oliveira-Brett, A.M., 2011a. Boron doped diamond and glassy carbon electrodes comparative study of the oxidation behaviour of cysteine and methionine. Bioelectrochemistry 81 (1), 46–52.

Enache, T.A., Oliveira-Brett, A.M., 2011b. Pathways of electrochemical oxidation of indolic compounds. Electroanalysis 23 (6), 1337–1344.

Enache, T.A., Oliveira-Brett, A.M., 2013. Peptide methionine sulfoxide reductase A (MsrA): direct electrochemical oxidation on carbon electrodes. Bioelectrochemistry 89, 11–18.

Enache, T.A., Chiorcea-Paquim, A.M., Oliveira-Brett, A.M., 2016. Amyloid-beta peptides time-dependent structural modifications: AFM and voltammetric characterization. Anal. Chim. Acta 926, 36–47.

Ferreira, A.A.P., Colli, W., Alves, M.J.M., Oliveira, D.R., Costa, P.I., Güell, A.G., Sanz, F., Benedetti, A.V., Yamanaka, H., 2006. Investigation of the interaction between Tc85-11 protein and antibody anti-T. cruzi by AFM and amperometric measurements. Electrochim. Acta 51 (24), 5046–5052.

Ferreira, L.F., Souza, L.M., Franco, D.L., Castro, A.C.H., Oliveira, A.A., Boodts, J.F.C., Brito-Madurro, A.G., Madurro, J.M., 2011. Formation of novel polymeric films derived from 4-hydroxybenzoic acid. Mater. Chem. Phys. 129 (1–2), 46–52.

Giancane, G., Consolaro, A., Lanni, S., Davi, S., Schiappapietra, B., Ravelli, A., 2016. Juvenile idiopathic arthritis: diagnosis and treatment. Rheumatol. Ther. 3 (2), 187–207.

Giancane, G., Alongi, A., Ravelli, A., 2017. Update on the pathogenesis and treatment of juvenile idiopathic arthritis. Curr. Opin. Rheumatol.

Han, L., Liu, C.M., Dong, S.L., Du, C.X., Zhang, X.Y., Li, L.H., Wei, Y., 2017. Enhanced conductivity of rGO/Ag NPs composites for electrochemical immunoassay of prostate-specific antigen. Biosens. Bioelectron. 87, 466–472.

Hennessey, H., Afara, N., Omanovic, S., Padjen, A.L., 2009. Electrochemical investigations of the interaction of C-reactive protein (CRP) with a CRP antibody chemically immobilized on a gold surface. Anal. Chim. Acta 643 (1–2), 45–53.

Hersh, A.O., Prahalad, S., 2015. Immunogenetics of juvenile idiopathic arthritis: a comprehensive review. J. Autoimmun. 64, 113–124.

Humphrey, W., Dalke, A., Schulten, K., 1996. VMD: visual molecular dynamics. J. Mol. Graph. 14 (1), 33–38 (27–38).

Hwang, H.J., Ryu, M.Y., Park, C.Y., Ahn, J., Park, H.G., Choi, C., Ha, S.D., Park, T.J., Park, J.P., 2017. High sensitive and selective electrochemical biosensor: label-free detection of human norovirus using affinity peptide as molecular binder. Biosens. Bioelectron. 87, 164–170.

Karunakaran, C., Rajkumar, R., Bhargava, K., 2015. Chapter 1 – Introduction to Biosensors. Biosensors and Bioelectronics. Elsevier, Amsterdam, pp. 1–68.

Lear, S., Cobb, S.L., 2016. Pep-Calc.com: a set of web utilities for the calculation of peptide and peptoid properties and automatic mass spectral peak assignment. J. Comput. Aided Mol. Des. 30 (3), 271–277.

Li, R., Huang, H., Huang, L., Lin, Z., Guo, L., Qiu, B., Chen, G., 2013. Electrochemical biosensor for epidermal growth factor receptor detection with peptide ligand. Electrochim. Acta 109, 233–237.

Liu, Q., Wang, J., Boyd, B.J., 2015. Peptide-based biosensors. Talanta 136, 114–127.

Liu, X., Marrakchi, M., Xu, D., Dong, H., Andreescu, S., 2016. Biosensors based on modularly designed synthetic peptides for recognition, detection and live/dead differentiation of pathogenic bacteria. Biosens. Bioelectron. 80, 9–16.

Luna, D.M., Oliveira, M.D., Nogueira, M.L., Andrade, C.A., 2014. Biosensor based on lectin and lipid membranes for detection of serum glycoproteins in infected patients with dengue. Chem. Phys. Lipids 180, 7–14.

Pakapongpan, S., Poo-Arporn, R.P., 2017. Self-assembly of glucose oxidase on reduced graphene oxide-magnetic nanoparticles nanocomposite-based direct electrochemistry for reagentless glucose biosensor. Mater. Sci. Eng. C Mater. Biol. Appl. 76, 398–405.

Pan, L.H., Kuo, S.H., Lin, T.Y., Lin, C.W., Fang, P.Y., Yang, H.W., 2017. An electrochemical biosensor to simultaneously detect VEGF and PSA for early prostate cancer diagnosis based on graphene oxide/ssDNA/PLLA nanoparticles. Biosens. Bioelectron. 89 (Pt 1), 598–605.

Pandey, A., Gurbuz, Y., Ozguz, V., Niazi, J.H., Qureshi, A., 2017. Graphene-interfaced electrical biosensor for label-free and sensitive detection of foodborne pathogenic E. coli O157:H7. Biosens. Bioelectron. 91, 225–231.

Pang, X., Pan, J., Gao, P., Wang, Y., Wang, L., Du, B., Wei, Q., 2015. A visible light induced photoelectrochemical aptsensor constructed by aligned ZnO@CdTe core shell nanocable arrays/carboxylated g-C3N4 for the detection of proprotein convertase subtilisin/kexin type 6 gene. Biosens. Bioelectron. 74, 49–58.

Paraíso, L.F., Paula, L.F., Franco, D.L., Madurro, J.M., Brito-Madurro, A.G., 2014. Bioelectrochemical detection of alanine aminotransferase for molecular diagnostic of the liver disease. Int. J. Electrochem. Sci. 9, 1286–1297.

Patris, S., Vandeput, M., Kenfack, G.M., Mertens, D., Dejaegher, B., Kauffmann, J.M., 2016. An experimental design approach to optimize an amperometric immunoassay on a screen printed electrode for Clostridium tetani antibody determination. Biosens. Bioelectron. 77, 457–463.

Pavan, S., Berti, F., 2012. Short peptides as biosensor transducers. Anal. Bioanal. Chem. 402 (10), 3055–3070.

Phillips, J.C., Braun, R., Wang, W., Gumbart, J., Tajkhorshid, E., Villa, E., Chipot, C., Skeel, R.D., Kalé, L., Schulten, K., 2005. Scalable molecular dynamics with NAMD. J. Comput. Chem. 26 (16), 1781–1802.

Rodrigues, L.P., Ferreira, L.F., Monte, A.F.G.d., Brito-Madurro, A.G., Madurro, J.M., 2014. Bioelectrode applied to diagnosis of cardiac disease. J. Nanosci. Nanotechnol. 14 (9), 6528–6538.

Sahin, M., Ayranci, E., 2015. Electrooxidation of NADH on modified screen-printed electrodes: effects of conducting polymer and nanomaterials. Electrochim. Acta 166, 261–270.

Sharma, M.K., Agarwal, G.S., Rao, V.K., Upadhyay, S., Merwyn, S., Gopalan, N., Rai, G.P., Vijayaraghavan, R., Prakash, S., 2010. Amperometric immunosensor based on gold nanoparticles/alumina sol-gel modified screen-printed electrodes for antibodies to Plasmodium falciparum histidine rich protein-2. Analyst 135 (3), 608–614.

Silva, J.V., Pimentel, D.M., Souto, D.E.P., Cássia Silva Luz, R., Damos, F.S., 2013. Application of horseradish peroxidase/polyaniline/bis(2-aminoethyl) polyethylene glycol-functionalized carbon nanotube composite as a platform for hydrogen peroxide detection with high sensitivity at low potential. J. Solid State Electrochem. 17 (11), 2795–2804.

Souto, D.E., Silva, J.V., Martins, H.R., Reis, A.B., Luz, R.C., Kubota, L.T., Damos, F.S., 2013. Development of a label-free immunosensor based on surface plasmon resonance technique for the detection of anti-Leishmania infantum antibodies in canine serum. Biosens. Bioelectron. 46, 22–29.

Souza e Silva, T.D., Castro, A.C.H., Rodovalho, V.R., Madurro, J.M., Brito-Madurro, A.G., 2016. Development of electrochemical genosensor for MYCN oncogene detection using rhodamine B as electroactive label. J. Solid State Electrochem. 20 (9), 2411–2418.

Villa, M.d.G., Jimenez-Jorquera, C., Haro, I., Gomara, M.J., Sanmarti, R., Fernandez-Sanchez, C., Mendoza, E., 2011. Carbon nanotube composite peptide-based biosensors as putative diagnostic tools for rheumatoid arthritis. Biosens. Bioelectron. 27 (1), 113–118.

Wang, H., Lei, C., Li, J., Wu, Z., Shen, G., Yu, R., 2004. A piezoelectric immunoagglutination assay for Toxoplasma gondii antibodies using gold nanoparticles. Biosens. Bioelectron. 19 (7), 701–709.

Wipff, J., Sparsa, L., Lohse, A., Quartier, P., Kahan, A., Deslandre, C.J., 2016. Impact of juvenile idiopathic arthritis on quality of life during transition period at the era of biotherapies. Jt. Bone Spine 83 (1), 69–74.

Yang, J., Yan, R., Roy, A., Xu, D., Poisson, J., Zhang, Y., 2015. The I-TASSER suite: protein structure and function prediction. Nat. Methods 12 (1), 7–8.